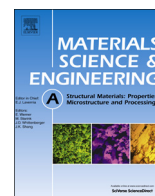




ELSEVIER

Contents lists available at ScienceDirect

Materials Science & Engineering A

journal homepage: www.elsevier.com/locate/msea

Anomalous stabilization of austenitic stainless steels at cryogenic temperatures

Michael Hauser^{a,*}, Marco Wendler^a, Olga Fabrichnaya^b, Olena Volkova^a, Javad Mola^a^a Institute of Iron and Steel Technology, TU Bergakademie Freiberg, 09599 Freiberg, Saxony, Germany^b Institute of Materials Science, TU Bergakademie Freiberg, 09599 Freiberg, Saxony, Germany

ARTICLE INFO

Article history:

Received 6 July 2016

Received in revised form

15 August 2016

Accepted 19 August 2016

Available online 21 August 2016

Keywords:

TRIP steel

Gibbs energy

Néel temperature

Mechanical stability

Austenitic steel

Martensitic transformation

ABSTRACT

The deformation-induced formation of α' martensite was investigated by tensile testing of a Fe-19Cr-3Mn-4Ni-0.15C-0.17N cast austenitic steel between -196 °C and 400 °C. The steel did not exhibit spontaneous α' martensite formation at temperatures as low as -196 °C. Therefore, the critical driving force for the formation of α' (-2780 J/mol) was obtained by determining the complementary mechanical energy necessary to trigger the deformation-induced α' martensite at 0 °C. Driving forces for the $\gamma \rightarrow \alpha'$ transformation at other tensile test temperatures associated with the deformation-induced α' formation were then obtained by subtracting the mechanical energies applied to trigger the martensitic transformation from the critical driving force. The triggering mechanical energies were obtained from in-situ magnetic measurements which enabled to mark the onset of the $\gamma \rightarrow \alpha'$ transformation. The driving forces for the $\gamma \rightarrow \alpha'$ transformation calculated using the preceding method indicated an increase in the stability of austenite which was attributed to changes in the mechanical and physical properties of austenite in the vicinity of the Néel temperature. The method can be used to calculate modified driving forces for the occurrence of the $\gamma \rightarrow \alpha'$ phase transformation.

© 2016 Elsevier B.V. All rights reserved.

1. Introduction

Thermodynamic modeling is a powerful tool in the design of engineering materials. It enables to calculate the Gibbs energies of phases in a given system and provides important information such as phase transformation temperatures [1–7]. For austenitic steels, the T_0 temperature at which the Gibbs energies of austenite and ferrite are equal could be obtained from thermodynamic calculations [3,8,9]. Furthermore, with the knowledge of the minimum thermodynamic driving force for the spontaneous martensite (α') formation, the martensite start (M_s) temperature too can be predicted [3,8,9].

Depending on the chemical composition and deformation temperature, deformation mechanisms such as dislocations cell formation, mechanical twinning, and martensitic transformation may occur in the austenite phase of high-alloy steels [10–20]. The martensite commonly forms at intersections of glide bands in the austenite. At low temperatures where martensite formation is enabled, glide bands may consist of stacking fault bundles, ϵ martensite, and mechanical twins [21,22]. In austenitic steels exhibiting the transformation-induced plasticity (TRIP) effect, the

knowledge of the minimum driving force necessary for the martensite formation is of primary importance. The concept of defining a critical driving force for the martensite nucleation was first put forward by Cohen and coworkers [23,24] and has been extended by Ghosh and Olson to include the effect of alloying elements [1]. The critical driving force ($\Delta G_{crit}^{\gamma \rightarrow \alpha'}$) is equal to the Gibbs energy of the martensitic transformation at the M_s temperature ($\Delta G_{chem}^{\gamma \rightarrow \alpha'}(M_s)$), namely $\Delta G_{crit}^{\gamma \rightarrow \alpha'} = \Delta G_{chem}^{\gamma \rightarrow \alpha'}(M_s)$.

As long as the M_s temperature is known, the critical driving force can be determined from the knowledge of the temperature dependence of the Gibbs energy. The accuracy of such calculations will then depend on the reliability of the thermodynamic data. The thermodynamic database is particularly trustworthy in the region where it has been supported by experimental data [3,4]. Especially at low temperatures, reliability of the thermodynamic data decreases because it is no longer possible to reach equilibrium within a reasonable time. Another factor contributing to the low reliability of thermodynamic databases at low temperatures is the antiferromagnetic-paramagnetic transition of austenite at Néel temperature [25–29]. In this paper, modified Gibbs energies for the $\gamma \rightarrow \alpha'$ transformation were obtained by tensile testing of an austenitic TRIP steel between -196 °C and 400 °C and the determination of the triggering stress for the martensitic transformation by in-situ magnetic measurements. The approach used in this

* Corresponding author.

E-mail address: Michael.Hauser@iest.tu-freiberg.de (M. Hauser).

work is applicable to other austenitic TRIP steels and may be used to enhance the existing thermodynamic databases.

2. Materials and methods

The investigated steel was melted in a vacuum induction furnace under a nitrogen partial pressure of 45 kPa before being cast into a water-cooled copper mould with a dimension of $230 \times 35 \times 95 \text{ mm}^3$. The chemical composition of the cast steel is given in Table 1. To avoid pore formation in ingots, the nitrogen partial pressure was raised to 150 kPa in the subsequent casting step.

The steel was machined to round tensile test specimens with a gauge diameter of 6 mm. To ensure the absence of machining-induced martensite near the surface of tensile specimens, the solution heat treatment was performed after machining. The solution heat treatment aimed at the dissolution of carbides and nitrides likely present in the as-cast microstructure. It also led to the partial homogenization of the steel in the austenite phase field. The solution heat treatment consisted of holding the steel at $1150 \text{ }^\circ\text{C}$ for 30 min under an argon atmosphere.

Quasi-static uniaxial tensile tests were performed using a Zwick 1476-type universal testing machine. The initial strain rate was $4 \times 10^{-4} \text{ s}^{-1}$. With the aid of a thermal chamber which surrounded the tensile specimen and its constraints, different temperatures in the range of $-196 \text{ }^\circ\text{C}$ to $400 \text{ }^\circ\text{C}$ could be adjusted.

For the ex-situ quantification of the ferromagnetic phase content in tensile specimens, a Metis MSAT-type magnetic saturation device equipped with a Lakeshore 480 fluxmeter was used. The equipment enabled the measurement of magnetic flux density after saturation magnetization of specimens cut from the gauge section of tensile specimens.

The microstructure was studied by means of electron channeling contrast imaging (ECCI) and electron backscatter diffraction (EBSD) techniques in a Zeiss LEO-1530 GEMINI-type field emission scanning electron microscope (FESEM).

An in-situ magnetic measurement system was devised to determine the triggering stress for the martensite formation during tensile tests. The magnetic measurement system consisted of two coils. The first coil served to generate an electromagnetic field which magnetized the martensite phase as it formed during tensile loading. The magnetization of martensite phase in tensile specimens induced an electrical potential difference (voltage) in the second coil which was recorded [30]. To calculate Gibbs energies for the austenite (fcc) and martensite (bcc) phases and the Néel temperature of austenite, the thermodynamic database developed by Franke et al. [31] was used. Calculations were done using the Thermo-Calc software [32].

3. Results and discussion

Fig. 1 shows the stress-strain curves for the tensile test specimens deformed until fracture at temperatures between $-196 \text{ }^\circ\text{C}$ and $400 \text{ }^\circ\text{C}$. The highest total elongation of 73% was reached at $60 \text{ }^\circ\text{C}$ which is almost equal to the M_d temperature, namely the highest temperature associated with the deformation-induced martensite formation. The formation of martensite at lower

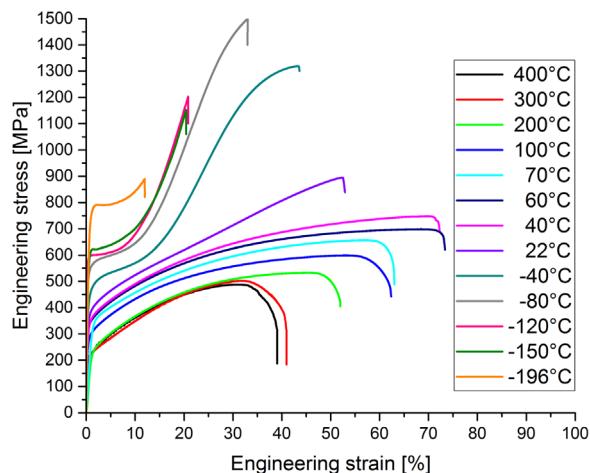


Fig. 1. Engineering stress-strain curves of tensile specimens in the temperature range of $-196 \text{ }^\circ\text{C}$ to $400 \text{ }^\circ\text{C}$.

temperatures resulted in a pronounced strengthening and a steady decrease in elongation. Reduction of tensile elongation at temperatures below the M_d temperature is a common occurrence in austenitic stainless steels [13,20,33,34]. The highest engineering stress level of 1500 MPa was reached at $-80 \text{ }^\circ\text{C}$. At deformation temperatures below $-80 \text{ }^\circ\text{C}$, tensile specimens failed at significantly lower stress levels. This could be related to the occurrence of surface decarburization/denitriding processes during the solution annealing. These processes enable the formation of a continuous martensite layer on the surface of tensile specimens thereby facilitating the nucleation of surface cracks [35,36].

To specify the deformation mechanisms activated during tensile tests, SEM and EBSD investigations were carried out on tensile specimens deformed until fracture at $-196 \text{ }^\circ\text{C}$ and $70 \text{ }^\circ\text{C}$ (Fig. 2). The prior tensile loading axis is horizontal in the micrograph. The ECCI micrograph of Fig. 2(a) shows the presence of a high density of nearly straight deformation bands in the microstructure of the specimen deformed at $-196 \text{ }^\circ\text{C}$. This indicates the dominance of planar glide due to the high activity of Shockley partial dislocations at $-196 \text{ }^\circ\text{C}$ [19]. According to the EBSD phase map of the specimen tested at $-196 \text{ }^\circ\text{C}$ (Fig. 2(c)), many of the deformation bands have transformed to martensite. Due to the coexistence of a small fraction of ϵ -martensite in the glide bands, the martensitic transformation has likely occurred according to the sequence $\gamma \rightarrow \epsilon \rightarrow \alpha'$. This sequence has been similarly observed in the Fe-16Cr-6Mn-6Ni (values in mass-%) stainless steel [13,37]. It is well established that the type of deformation-induced processes in austenitic steels depends on the stacking fault energy; as the stacking fault energy decreases, the deformation mechanism changes from perfect dislocations glide to deformation twinning, ϵ -martensite formation, and α' martensite formation in that sequence [38]. The dominance of α' and ϵ martensite at the expense of twinning after deformation at $-196 \text{ }^\circ\text{C}$ (Fig. 2(c)) is in agreement with the reduction in the stacking fault energy at lower temperatures [39].

The ECCI micrograph of the specimen tensile tested at $70 \text{ }^\circ\text{C}$ (Fig. 2(b)) shows two austenite grains with different microstructural characteristics. Whereas the microstructure of the austenite grain to the left resembles the microstructure shown in Fig. 2(a), diffuse contrast changes in the austenite grain to the right imply the dominance of wavy glide [17,18,40]. Abrupt transition in the glide mode across a grain boundary is more consistent with the differences in the crystallographic orientation of the neighboring grains than with the possible segregation of alloying elements in the cast steel. After all, the forces exerted on the leading and trailing partial dislocations of the primary slip system depend

Table 1
Chemical composition of the investigated cast steel in mass-%.

Alloy	C	N	Cr	Mn	Ni	Si	Fe
Cr19NC17.15	0.154	0.167	18.70	2.94	4.22	0.52	bal.

Download English Version:

<https://daneshyari.com/en/article/1573050>

Download Persian Version:

<https://daneshyari.com/article/1573050>

[Daneshyari.com](https://daneshyari.com)